Supplementary Information (SI) for Journal of Materials Chemistry B.

Supplementary Data

Lyophilized Tumour Cell-Loaded ^{10}B-Doped Carbon Dots for Simultaneous Boron Neutron Capture Therapy and Enhancement of Antitumor Immunity of Prostate Cancer

Yongjin Yang,[a,b] Zhiyi Zhao,[c] Chengyu You, [a,b] Miao Pang,[d] Tianyuan Zhong,[d] Qingchao Li,[a,b] Shiwei Jing,[e] Yanxin Qi,*[d] Yubin Huang*[d] and Zhilong Dong*[a,b]

[a] Department of Urology, The second Hospital & Clinical Medical School, Lanzhou University, Lanzhou, 730000, Gansu, China.

[b] Gansu Province Clinical Research Center for Urinary system disease, Lanzhou, 730000, Gansu, China.

[c] Department of Andrology, First hospital of Jilin University, Changchun,130021, Jilin, China.

[d] Faculty of Chemistry, Northeast Normal University, Changchun, 130024, Jilin,China

[e] School of Physics, Northeast Normal University, Changchun, 130024, Jilin,China

* Corresponding author. E-mail: qiyx001@nenu.edu.cn(Y.Qi), huangyb350@nenu.edu.cn(Y.Huang) and dzl19780829@163.com(Z.Dong)

Chemicals and reagents

^{10}BA（≥95%）(Dalian Boronten Sci&Tech Co., Ltd.), Bovine Serum Albumin V (Beijing Solarbio Science & Technology Co., Ltd.), Cell Ferrous Iron (Fe^{2+}) Fluorometric Assay Kit (Elabscience Biotechnology Co., Ltd.), Reactive Oxygen Species Assay Kit and JC-1 Mitochondrial Membrane Potential Assay Kit (Yeasen Biotechnology (Shanghai) Co., Ltd.). Cell Meter™ Intracellular GSH Assay Kit（AST Bioquest Co., Ltd.）, Lipid Peroxidation Assay Kit with BODIPY 581/591 C11 and DNA Damage Assay Kit by γH2AX Immunofluorescence (Mouse Monoclonal Antibody and Green Fluorescence) (Beyotime Biotechnology). TNF-α and IFN-γ (Shanghai Langton Biotechnology Co., Ltd.). Actin and γH2AX antibodies purchased from Wuhan servicebio technology CO., LTD. Mouse splenic lymph isolation kit (Tianjin Hao Yang Biological Products Technology Co., Ltd.). FITC-anti-mouse CD3 Antibody, PE-anti-mouse CD4 antibody and APC-anti-mouse CD8 antibody (Biolegend). All reagents are not purified for direct use unless otherwise mentioned. The morphology of CDs is characterized by JEM-2100F field emission transmission electron microscope. The powder XRD patterns of ^{10}B-CDs were obtained by Smartlab X-ray powder diffractometer. The infrared spectra of ^{10}B-CDs were obtained by Bruker VERTEX 70 Fourier transform infrared spectrometer. The F-4600 fluorescence spectrometer (Hitachi, Japan) was used to detect the excitation and emission wavelengths of samples. The boron content of the ^{10}B-CDs was analyzed by an inductively coupled plasma emission spectrometer (ICP-AES, Prodigy). The X-ray photoelectron spectrometer (SHIMADZU AXIS SUPRA+) determines the properties of the sample surface. Agilent NovoCyte performed flow cytometry analysis. Cell fluorescence images and tissue images were captured by BioTek Cytation5.5. Laser Scanning Confocal Microscope (Olympus, FV-3000) was also used to capture cell fluorescence images. Animal tissues were imaged by CRI Maertro 500FL.

Regulatory

All the animal experiments were carried out with review and approval from the Animal Welfare and Ethics Committee of the School of Chemistry, Northeast Normal University (No.202402042).

Neutron Source

The neutron source used in this study (NT503) was provided by Professor Shiwei Jing from the College of Physics, Northeast Normal University. After processing with lead blocks, thermal neutrons can be obtained. Theoretically, the neutron output is 5.4 × 10^9 n s^{-1}, with a neutron exit distance of 9.9 cm from the target, and the radius of the circular exit surface is 0.55 cm. The Monte Carlo simulation (MCNP5) is as follows:

$$H = \frac{\Phi i \times Y \times T \times S}{Ki} \quad (1)$$

H represents the dose at the tumor site, *Φi* is the neutron flux in different energy ranges, *Y* is the neutron yield, *T* is the irradiation time, *S* is the tumor area, and *Ki* is the flux-to-dose conversion factor for different energy ranges.

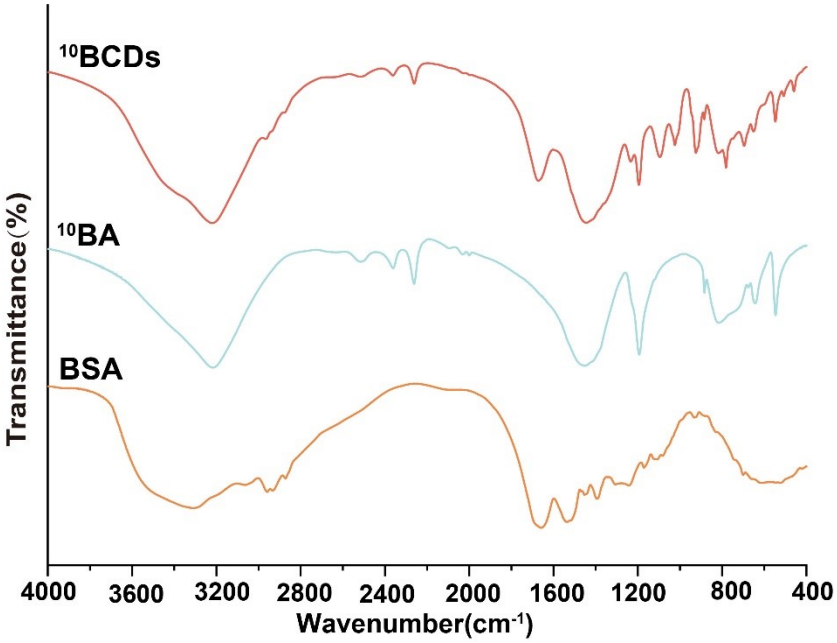

Fig.S 1 FT-IR spectra of ^{10}B-CDs, ^{10}BA and BSA

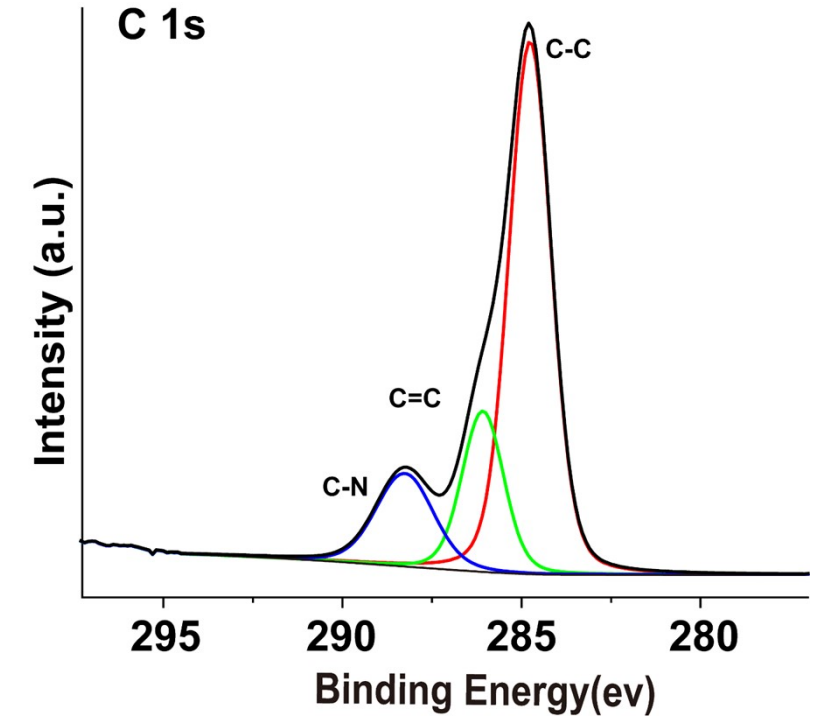

Fig.S 2 The high resolution XPS spectra of ^{10}B-CDs for C1s

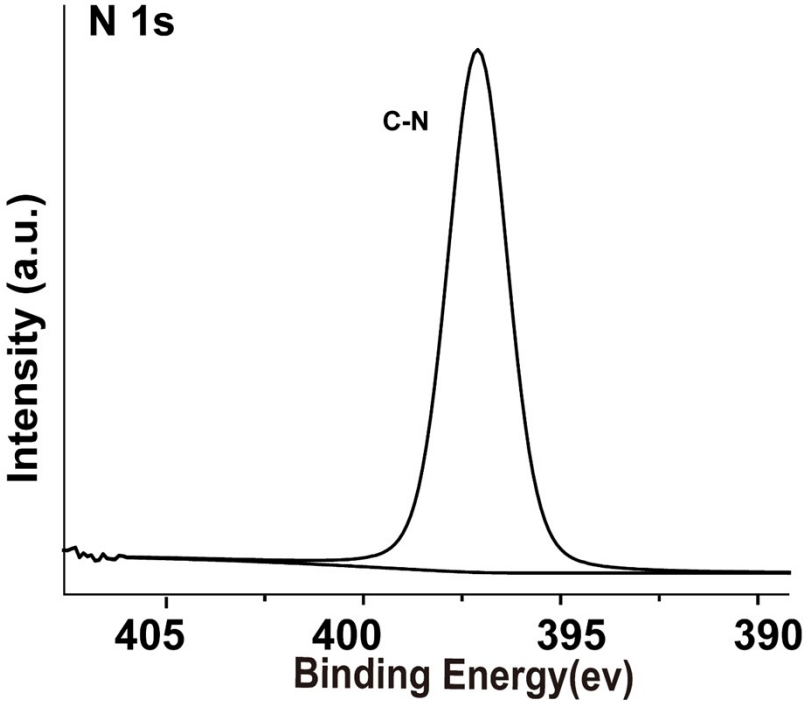

Fig.S 3 The high resolution XPS spectra of ^{10}B-CDs for N1s

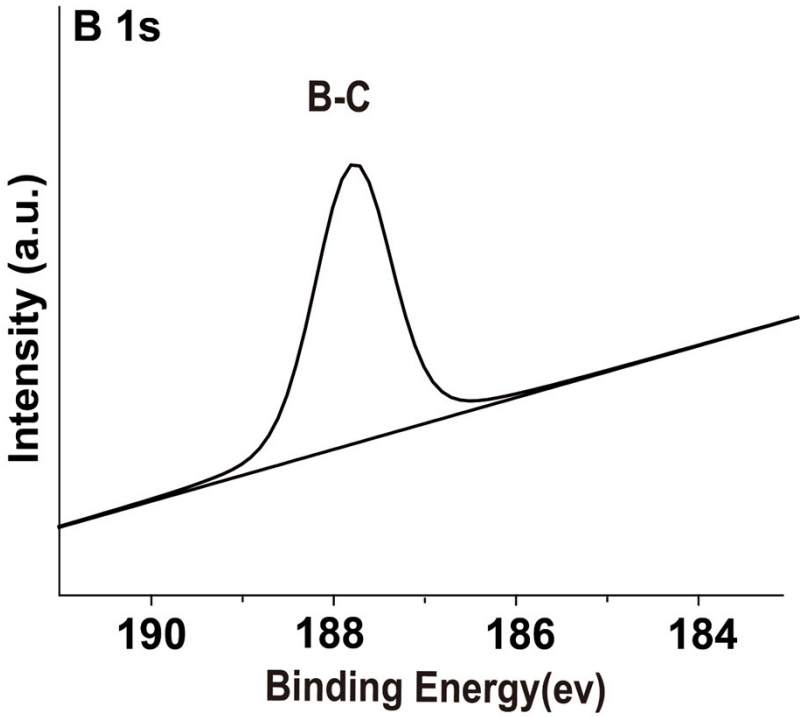

Fig.S 4 The high resolution XPS spectra of ^{10}B-CDs for N1s

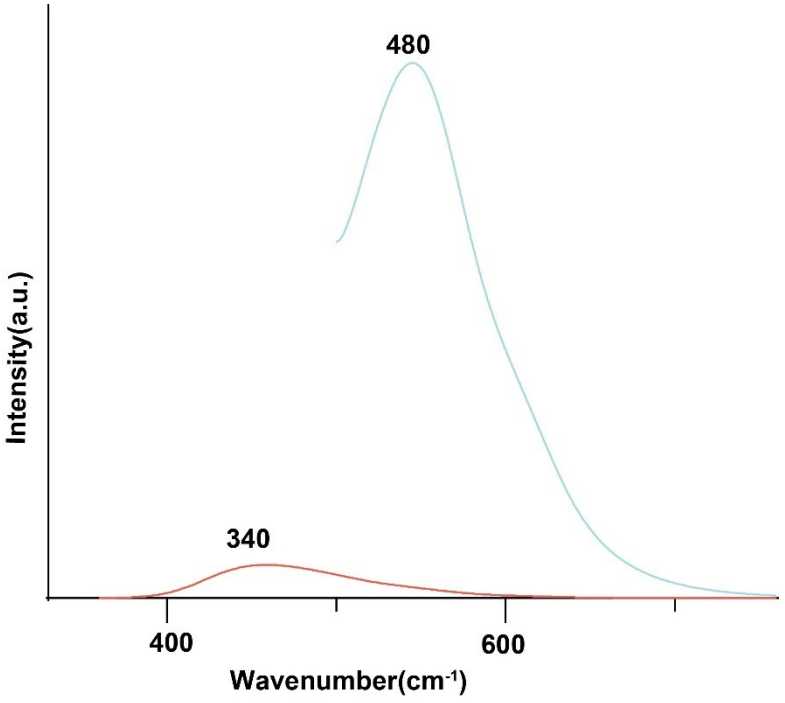

Fig.S 5 Fluorescence emission spectra of ^{10}B-CDs with different excitation wavelengths from 340 and 480 nm.

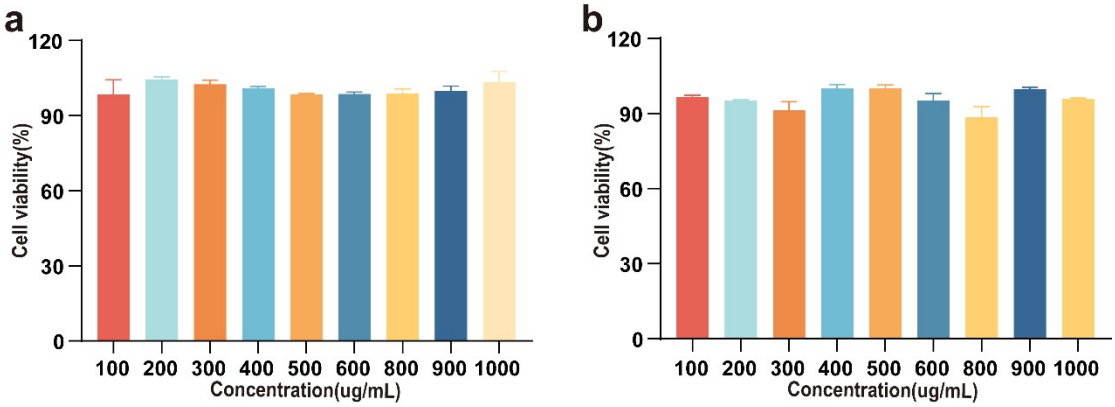

Fig.S 6 Cell viabilities of a) RM1 cells b) L929 cells treated with ^{10}B-CDs.

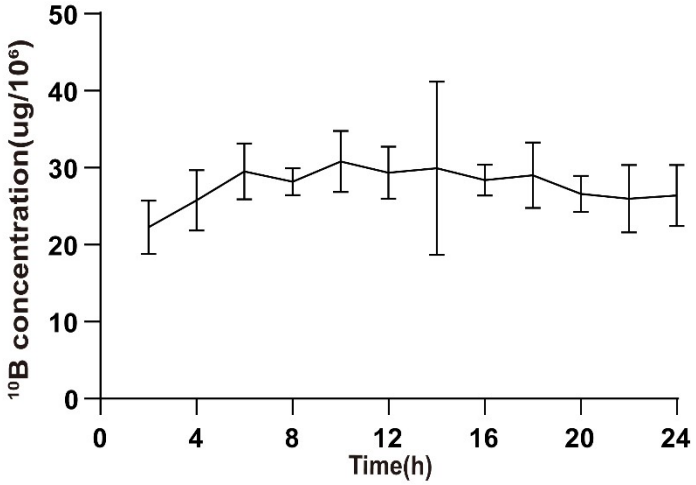

Fig.S 7 ^{10}B concentration in RM1 cells co-incubated with ^{10}B-CDs (400μg mL^{-1}) in different time.

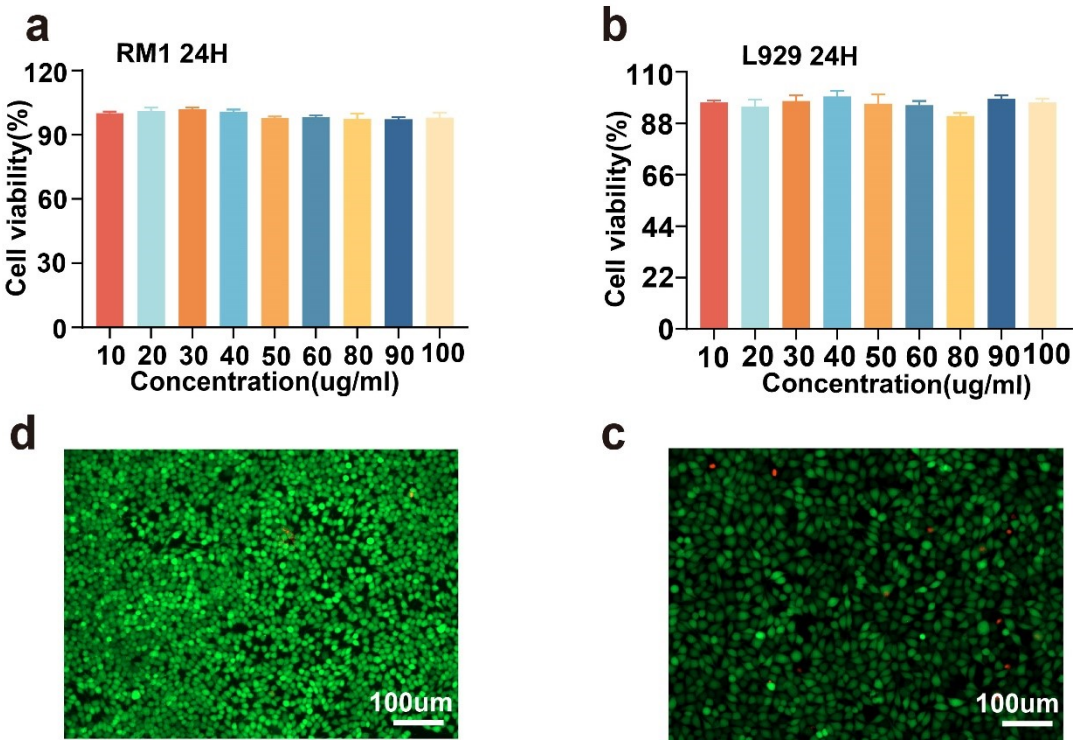

Fig.S 8 Cell viabilities of a) RM1 cells b) L929 cells treated with L-RM1@^{10}B-CDs. Calcein-AM/PI images of RM-1 cells(c) L929 cells (d)incubated with 100ug ml^{-1} of L-RM1@^{10}B-CDs

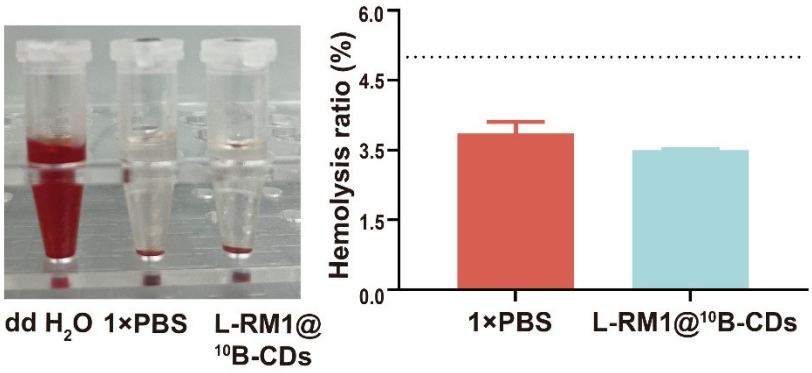

Fig.S 9 Images of hemolysis tests with 100 ug/mL L-RM1@^{10}B-CDs.

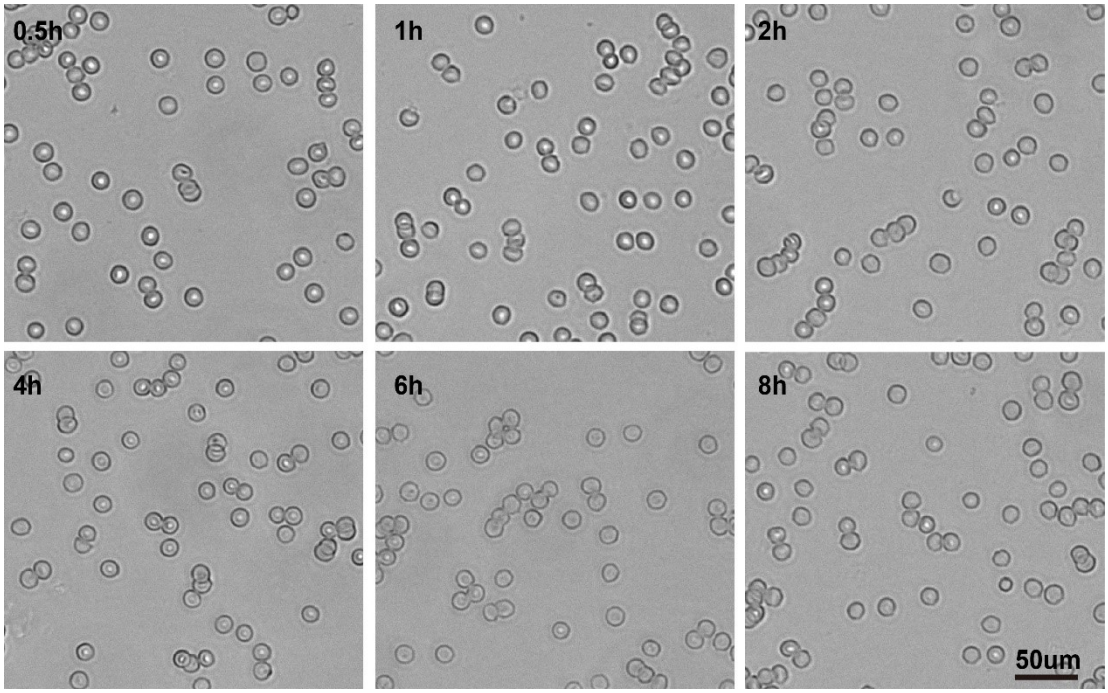

Fig.S 10 Images of red blood cell morphology after co-incubation of 100 ug/mL L-RM1@^{10}B-CDs.

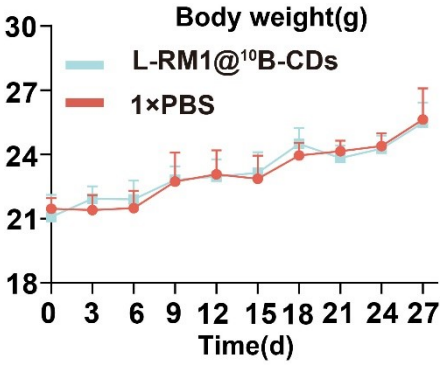

Fig.S 11 Body weight of C57BL/6 mice after treated with 15 mg kg^{-1} ^{10}B L-RM1@^{10}B-CDs.

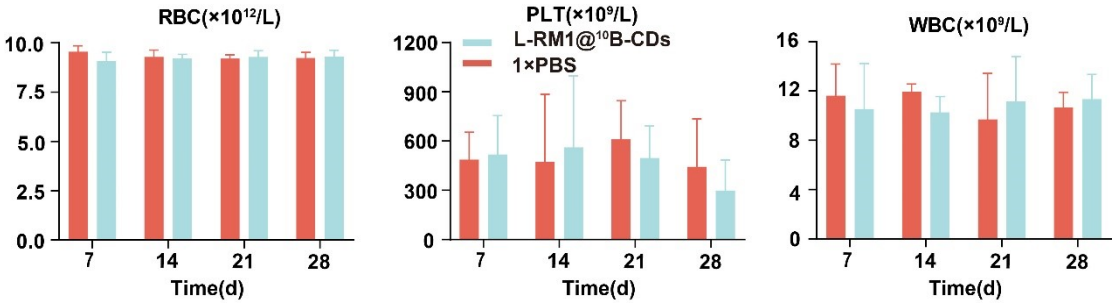

Fig.S 12 Hematological date of C57BL/6 mice after treated with 15 mg kg^{-1} ^{10}B L-RM1@^{10}B-CDs.

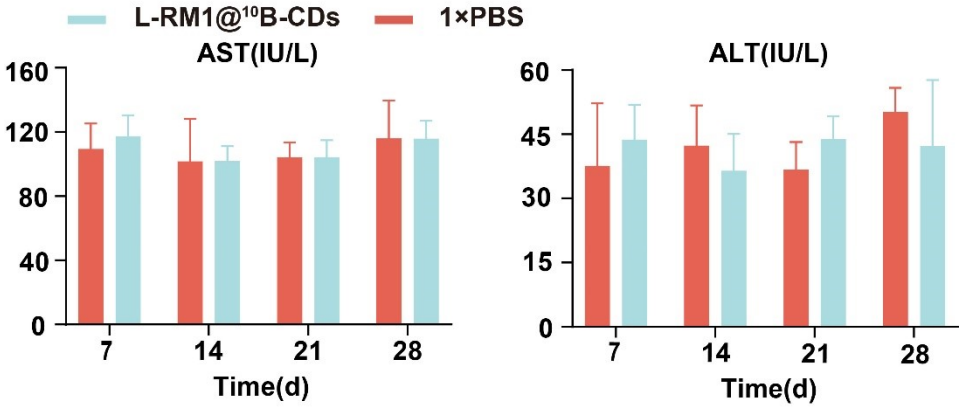

Fig.S 13 Liver function of C57BL/6 mice after treated with 15 mg kg^{-1} ^{10}B L-RM1@^{10}B-CDs.

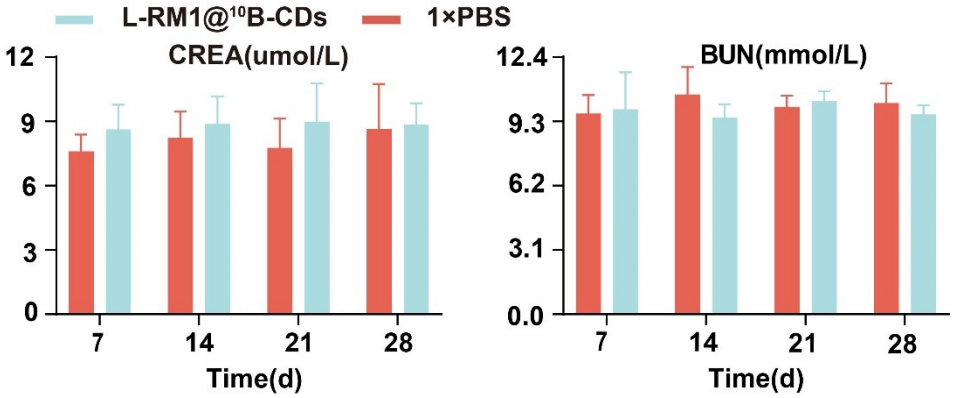

Fig.S 14 Kidney function of C57BL/6 mice after treated with 15 mg kg^{-1} ^{10}B L-RM1@^{10}B-CDs.

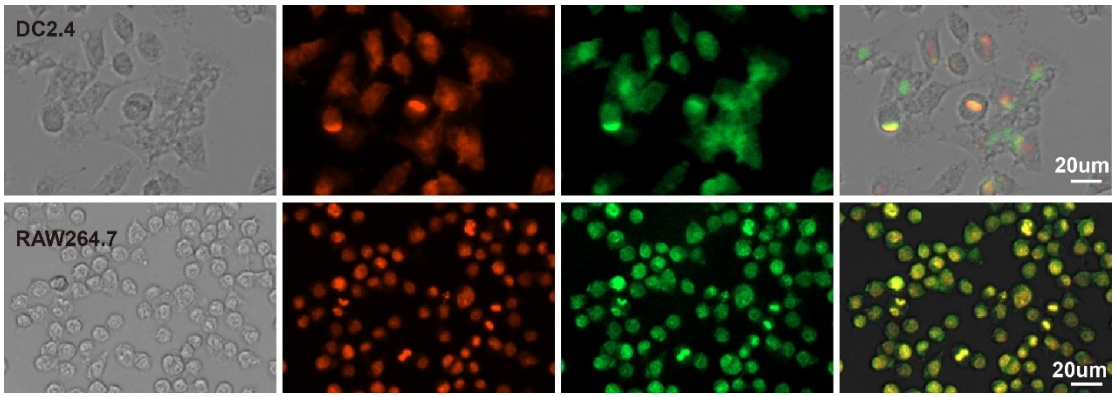

Fig.S 15 The uptake of DC2.4, Raw 264.7 cells after incubated with L-RM1@^{10}B-CDs (Cell membranes were labeled with DIR and ^{10}B-CDs with FITC) 8h.

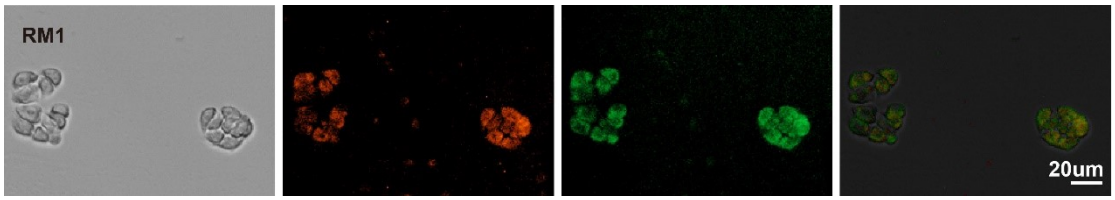

Fig.S 16 The uptake of RM1 cells after incubated with L-RM1@^{10}B-CDs (Cell membranes were labeled with DIR and ^{10}B-CDs with FITC) 8h.

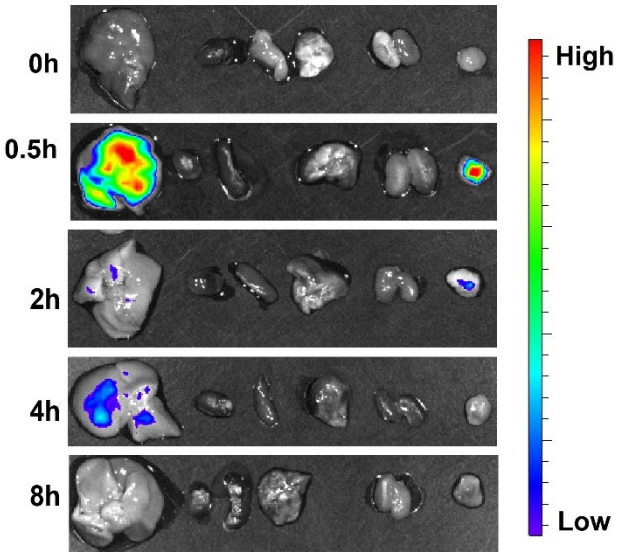

Fig.S 17 *Ex vivo* fluorescence images of the tumors and organs harvested from the mice bearing RM-1 tumors at different time points post-injection of ^{10}B-CDs.

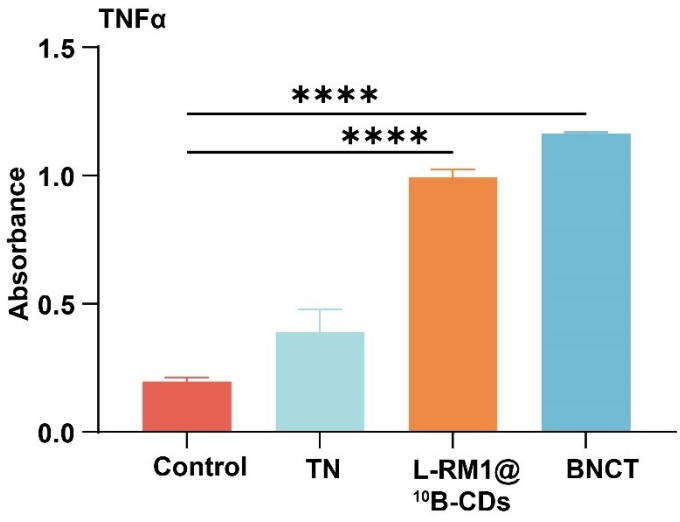

Fig.S 18 Cytokines TNFα in serum after treated with different methods.

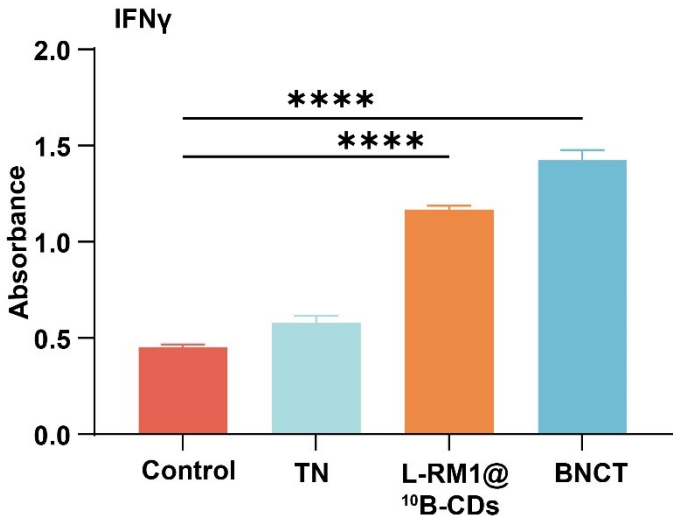

Fig.S 19 Cytokines IFNγ in serum after treated with different methods.

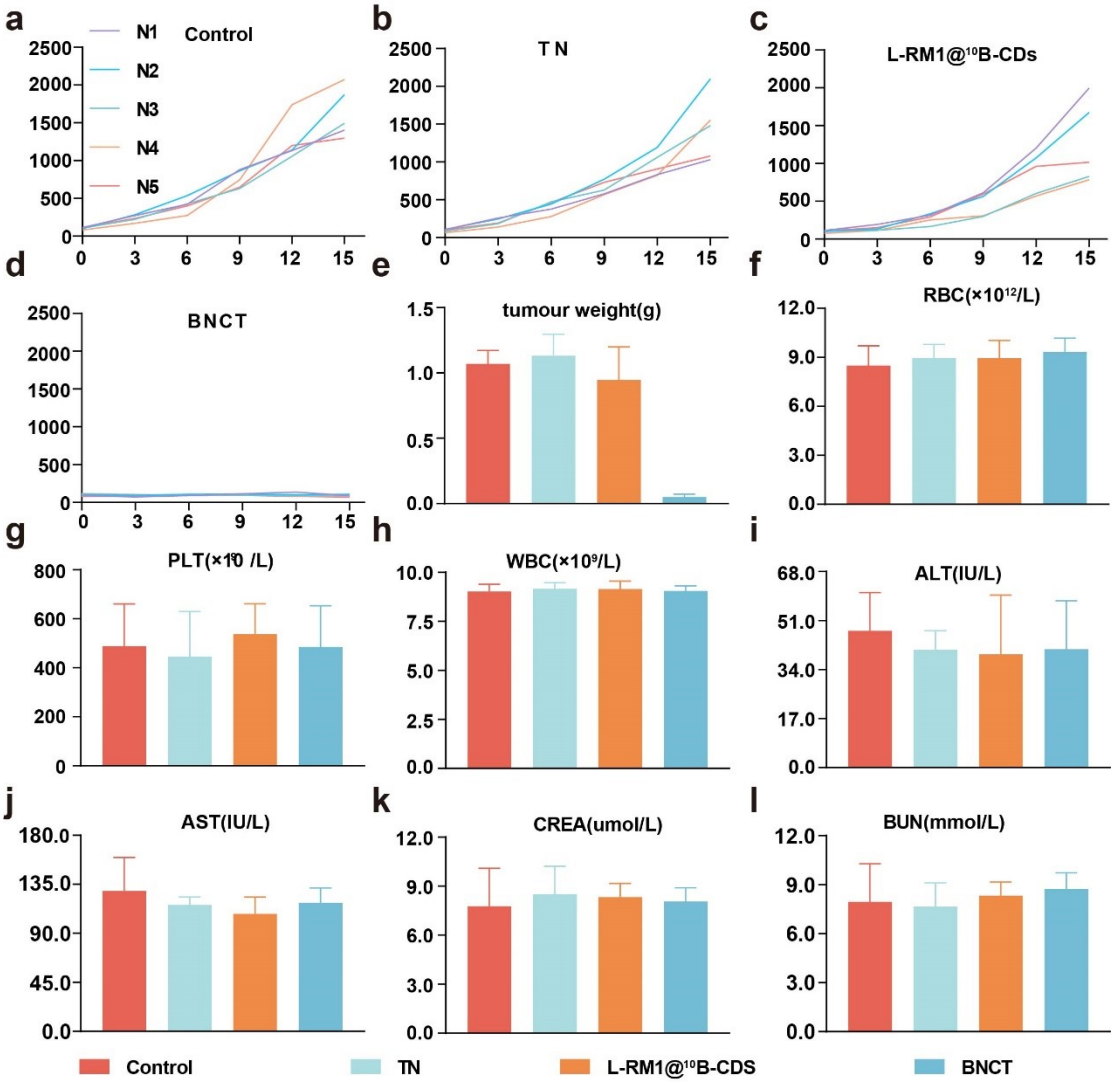

Fig.S 20 a-d) Tumor volume of RM-1 in C57BL/6 mice after treated with different methods. e) Tumor weight harvested from the mice bearing RM-1 tumors after being

treated with different methods. f-h) Hematological data of C57BL/6 mice bearing RM-1 tumors after being treated with different methods. i-j) Liver function of C57BL/6 mice bearing RM-1 tumors after being treated with different methods. k-l) Kidney function of C57BL/6 mice bearing RM-1 tumors after being treated with different methods.

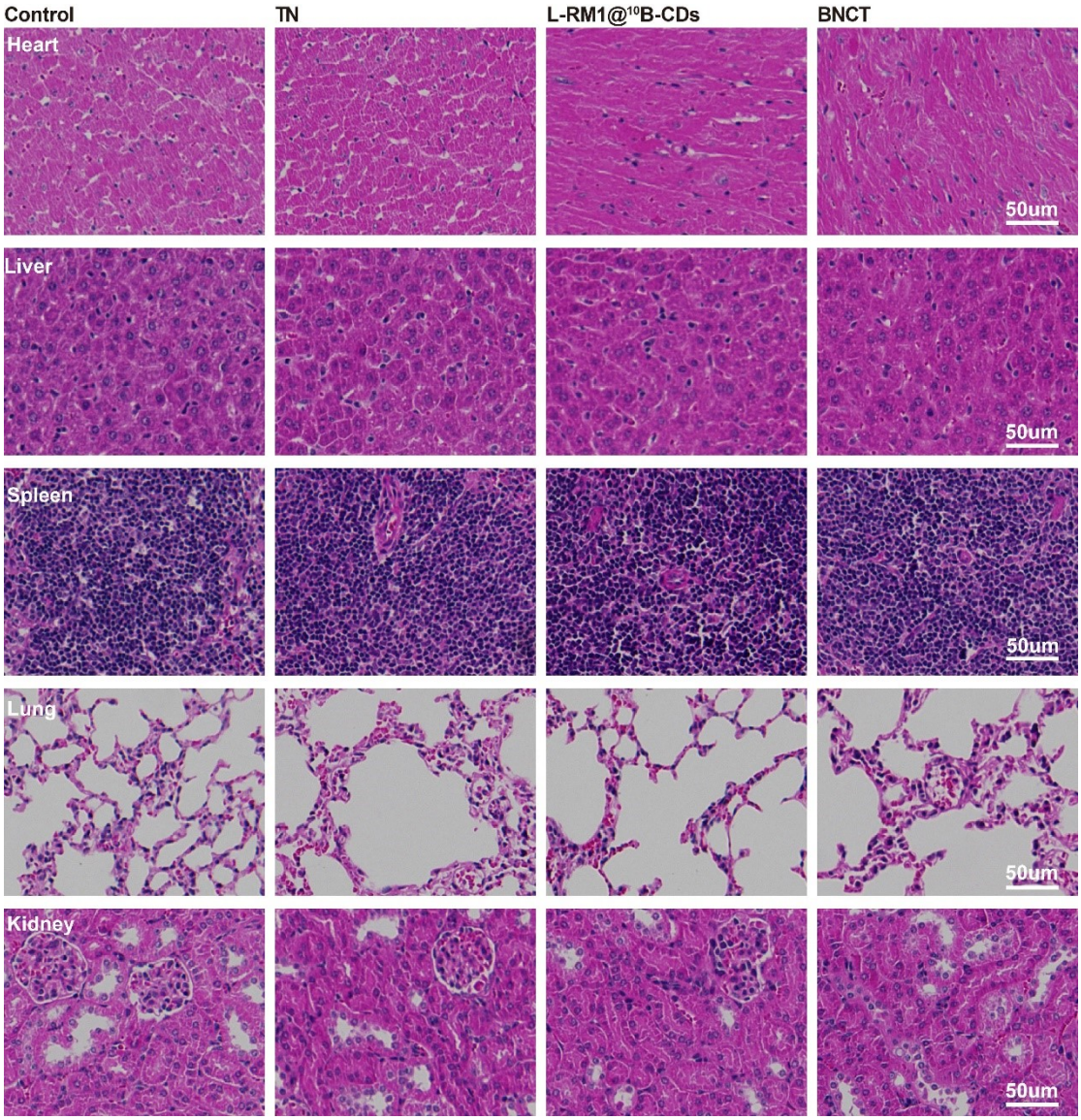

Fig.S 21 Representative H&E staining of major organs of RM1 tumor-bearing mice after various treatments.

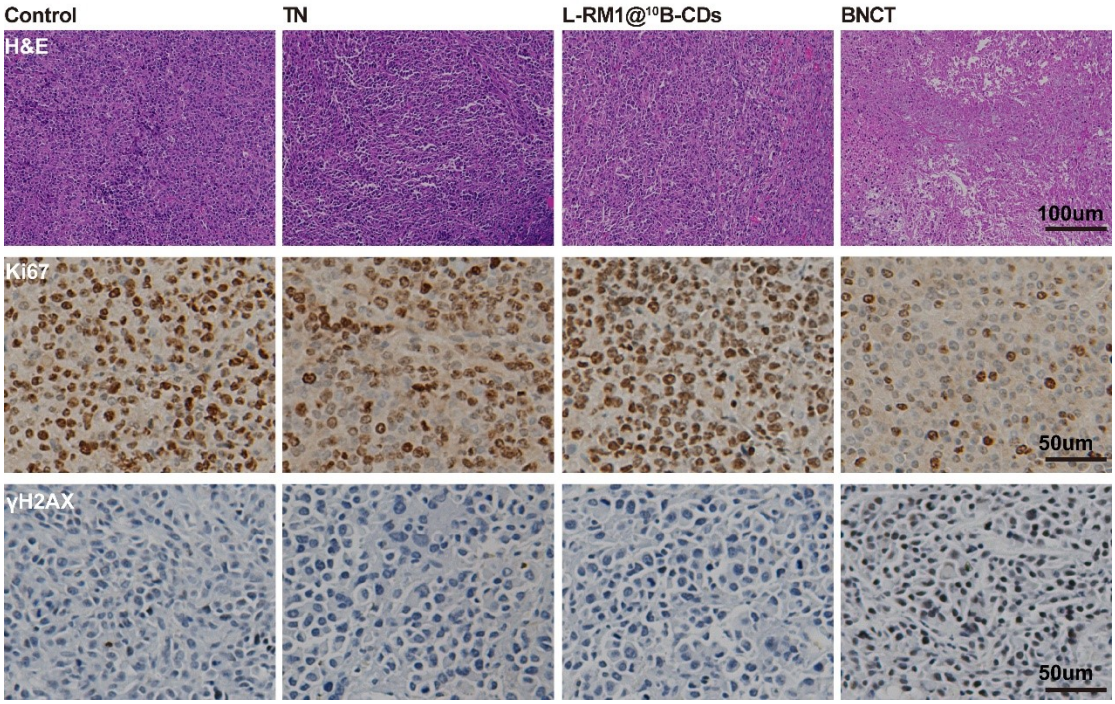

Fig.S 22 Representative H&E staining, Ki67 and γH2AX immunohistochemistry of tumor tissue after various treatments.